Mössbauer Effect Study of the Fe Spin Structure in Exchange-Bias and Exchange-Spring Systems

W. Keune, V.E. Kuncser[*], M. Doi[**], M. Askin , H. Spies, B. Sahoo, E. Duman and M. Acet
Institut für Physik, Gerhard-Mercator-Universität, D-47048 Duisburg, Germany

and

J.S. Jiang and S.D.Bader
Materials Science Division, Argonne National Laboratory, Argonne, IL 60439, USA

Abstract

Theoretical and experimental issues connected with exchange-bias and exchange-spring behavior are briefly reviewed, and the potential of conversion electron Mössbauer spectroscopy (CEMS), including the ^{57}Fe probe layer technique, to reveal the spin structure in layered systems is emphasized. First experimental results are reported for the new exchange-bias system $FeSn_2$/Fe and for the exchange-spring system Sm-Co/Fe.

I. Introduction

Pinning effects in bilayer magnetic systems with different magnetic anisotropy of the constituent layers give rise to interesting physical phenomena with important potential applications. Between them, a key attention is presently paid to the exchange bias and exchange spring phenomena.

Exchange bias phenomena are related to the unidirectional anisotropy induced at the interface between a soft ferromagnetic (FM) and an antiferromagnetic (AF) material with high magnetic anisotropy, when the system is prepared in a magnetic field or cooled down in an applied magnetic field through the Neel temperature, T_N, of the AF phase ($T_N < T_C$). Even though this effect was discovered in 1956 [1], its microscopic origin has not yet been fully understood, and the available theoretical models explain usually only the physical consequences of such an effect. Recent application of exchange biased thin films as magnetic recording media [2-4], domain stabilizers in recording heads [5-7] and especially "spin valve" devices [8-11] have renewed the interest in this effect and its underlying physics.

The main characteristics of the interface coupling due to the exchange anisotropy are [12]: (i) a shift of the hysteresis loop of the AF-FM system, generally in the opposite direction of the cooling field and known as exchange bias field, B_E , (ii) an additional sin component to the torque magnetization, with   the angle between the applied field and the cooling field direction, and (iii) a non-vanishing rotational hysteresis even at high fields. All these characteristics disappear at a temperature T_B , named blocking temperature, generally close to T_N . The coercivity in such systems becomes higher after inducing the exchange bias effect. Intuitively, the unidirectional anisotropy can be understood by assuming an exchange interaction at the AF-FM interface. By this interaction the AF spins exert a microscopic torque on the FM spins, keeping them longer

in the original position under the action of the applied field. The system behaves as being the subject of an additional internal biasing field which may also explain the shift of the hysteresis field. In spite of this simple phenomenological model, there is incomplete quantitative understanding of the above mentioned phenomena, and the role of the different parameters involved in the exchange bias mechanism (anisotropy, roughness, magnetic domains, etc.) is far from being fully understood.

The exchange spring phenomena are related to the pinning of a soft magnetic (SM) phase by a hard magnetic (HM) phase via exchange interactions acting at the interface between the two phases in contact. The hard magnetic phase provides the system with a high anisotropy and coercivity, whereas the soft magnetic phase enhances the saturation magnetization. Due to their unusual high remanence , large energy product and low cost [13-16], exchange spring magnets have attractive potential as permanent magnets. Usually they are used in the form of nanocomposites. Micromagnetic calculations and experimental results have shown that the exchange coupling depends on the grain size of the two phases, and that the intrinsic coercivity and the magnetic remanence are linearly reduced by increasing the amount of the soft phase [14,17]. In fact, nanocomposite materials are very complex systems and the presently available theoretical models fail in the quantitative description of the macroscopic parameters of exchange coupled nanocomposite magnets. In this respect, HM/SM bilayer films provide simple and convenient models for studying the microscopic spin structure related to exchange spring behaviour. On the other hand, a giant energy product may be expected in superlattices consisting of soft magnetic layers with high magnetization exchange that are coupled to aligned hard magnet layers.

This paper reviews briefly some theoretical and experimental issues connected with exchange bias and exchange spring behaviour and emphasizes the potential of conversion electron Mössbauer spectroscopy (CEMS), including the ^{57}Fe tracer layer technique, to reveal the spin configurations in layered systems with different magnetic anisotropy. Some experimental results are reported for two systems, namely $FeSn_2$/Fe and Sm-Co/Fe.

II.   Theoretical aspects and experimental issues

II.1. Exchange bias phenomena

In their early theory Meiklejohn and Bean supposed that the unidirectional anisotropy is due to the exchange coupling across an ideal interface between fixed and uncompensated AF spins and interfacial FM spins [1,18,19]. By minimizing the interface magnetic energy the model succeeded to explain the necessity of a strong in plane anisotropy of the AF spins in order to achieve the bias effect, but failed in the prediction of the magnitude of the loop shift, B_E . Order of magnitude higher values than the experimental ones were obtained. The main limitation of the above model was the supposition of a perfectly flat and uncompensated interface layer of the AF. Contrary, the experiments have shown similar exchange bias fields for both compensated and uncompensated AF interfaces. Therefore, reduced values for H_E compared with the prediction of the above model were subsequently explained by several additional effects, such as the formation of domain walls parallel to the interface [20,21] or roughness

leading to partial compensation by the presence of both AF sublattices along the interface [20]. The first theory which successfully described most of the phenomena related to B_E for both compensated and uncompensated interfaces was Molozemoff''s random-field model [22]. He explained the coupling as due to a random field attributed to interface roughness and to the formation of domain walls perpendicular to the interface in the AF phase when the system is cooled down through the Neel temperature. Characteristic to this model is that in spite of a strong atomistic interfacial exchange, the FM layer as a whole is not strongly pinned, because of the competition and cancellation of the random exchange directions. Unfortunately, the model failed to explain the large coercivity and the rotational hysteresis as well as a recent experimental finding, namely the tendency of the FM spins to align perpendicular to the AF easy axis [23,24]. Using a localized atomic spin model and forcing the antiferromagnetic spins to lie only in the film plane, Koon demonstrated the possibility of the perpendicular alignment between the FM and AF spins due to their frustration at the interface [25]. He showed also that rotational hysteresis could result from irreversible motions of the domain walls in the antiferromagnet. Schulthess and Butler have subsequently shown by a microscopic Heisenberg model including magnetostatic interaction and a higher degree of freedom for the interfacial spins, that the spin-flop coupling gives rise to a uniaxial anisotropy (which in turn causes the observed large coercivity), whereas the unidirectional anisotropy originates from interfacial defects [26]. By microscopical modeling of exchange bias Nowak, Misra and Usadel have introduced the domain state model [27]. Their simulations reveal the formation of magnetic domains in the antiferromagnetic part of the interface. These domains become frozen during the initial cooling procedure and carry a remanent net magnetization which causes the exchange bias. Clearly, there are several possible coupling mechanisms leading to exchange bias, and up to now even the most complex models have attained only partial degrees of agreement with the experimental results.

From the experimental point of view the macroscopic parameters related to the exchange bias effects have been investigated by various conventional techniques, excellently reviewed by Nogues and Schuller [12]. We like to emphasize that one of the main limitations for the atomistic description of exchange bias is related to the extension of the bulk antiferromagnetic spin configuration to the AF/FM interface in theoretical models; this may be not true due to the reduced coordination and symmetry, roughness or microstructural changes present in the contact area. Therefore, the knowledge of the real spin structure at the interface becomes a very important issue for understanding the microscopic mechanism of the exchange bias effect. Only very few studies on the local spin configuration at the interface have been reported, as analyzed by neutron diffraction [28] and very recently by X-ray magnetic dichroism in photoemission microscopy [29].
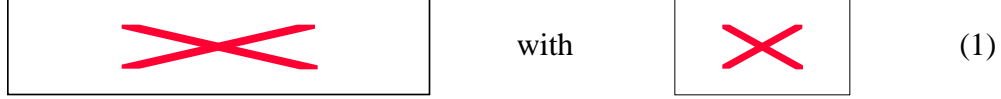
II.2 Exchange spring behaviour in layered systems

The spin reversal process in a SM film ferromagnetically coupled to a HM layer with uniaxial in-plane anisotropy was initially studied by Goto et al. [30] under the assumption that the hard layer is perfectly rigid and the soft layer has no anisotropy. For a thick enough soft layer (t > 50 nm), the spins in the soft layer remain parallel to the hard layer for applied fields less than an exchange field B_{ex}, which depends on the exchange

interaction, the thickness and the saturation magnetization of the soft magnetic layer. At higher fields, the spins in the soft layer are assumed to form an in-plane spiral spin structure, with the rotation angle increasing with distance from the hard layer. For a much thinner soft layer, this layer is expected to be rigidly coupled to the hard layer, both switching at a nucleation field, which depends on the geometrical and magnetic characteristics of both layers. In real situations, the soft layer may have a finite anisotropy and an intermediate thickness between the two situations described above. In such cases the hysteresis loops show both an exchange field, B_{ex}, where the spins in the soft layer start to rotate towards the applied field direction and an irreversible field, B_{irr}, where the hard layer switches irreversibly [31]. For the general case, more realistic theoretical results were obtained by analyzing the bilayer structure as a one-dimensional chain of spins normal to the layers. The final angular spin configuration was obtained by an iterative process based on the energy minimization procedure under the assumption that even deeper spins in the hard layer are allowed to rotate in the film plane [32-34]. According to this model, between the exchange field and the irreversible field, a spiral spin structure which extends across the whole soft-layer thickness and extends partially into the hard layer is formed. In spite of these recent achievements, no *direct* experimental observation of the spin structure in the soft magnetic layer has been reported.

III.   Determination of spin structure in layered systems by Mössbauer spectroscopy.

Compared with the other few techniques for studying interfacial spin structures, Mössbauer spectroscopy provides not only the spin structure, but simultaneously also the related metallurgical phases as well as information about the local structure and symmetry. These can be analysed with a high depth selectivity by using conversion electron Mössbauer spectroscopy (CEMS), combined with the tracer layer technique, using isotopically enriched ^{57}Fe probe layers (resolution limit of less than 1nm) at the interface or at different depths [35-37]. The only limitation for a suitable study of the spin structure is that the analyzed system should contain iron atoms with reasonably large magnetic moments, giving rise to high enough magnitudes of the hyperfine fields in order to resolve properly the line intensity ratios in the Mössbauer spectra. The spin configuration can be analyzed starting from the intensity ratio between the second (or fifth) and the third (or fourth) line, $R_{23} = I_2/I_3$, of the Zeeman-split Mössbauer sextet [38]. If the hyperfine field (which is anti-parallel to the spin direction) of an Fe atom is directed at an angle   vs. the Mössbauer -ray direction, then $R_{23}=4\sin^2$ $/(1+\cos^2$ $)$. It is observed that for in-plane distributed spins analyzed with incident -radiation perpendicular to the sample plane (=   = 90°), the above intensity ratio is insensitive to the in-plane spin direction ($R_{23} = 4$). Therefore, the spin configuration in layered samples with predominantly in-plane iron spins may be analyzed in non-perpendicular geometry with the radiation incident at an angle   vs. the sample plane (Fig.1). If the spin direction follows a certain angular distribution, P( ) , in the sample plane (where is the azimuthal angle), the intensity ratio may be expressed by the relationship[39]:

$$\boxed{} \qquad \text{with} \qquad \boxed{} \qquad (1)$$

The above intensity ratio can be theoretical evaluated for different model spin distributions as a function of the distribution parameters and the relative orientation between the sample and the radiation. The distribution parameters are evaluated by equating the theoretical expression to the experimental intensity ratio for a number of experimental values equal to the number of the distribution parameters [39]. For the simple case of a step-shape angular spin distribution (where the in-plane Fe spins are homogeneously distributed in a fan-like manner), the angular spin aperture may be estimated from only one Mössbauer spectrum.

A complete analysis of the spin structure at the interface is obtained by a first measurement in perpendicular geometry in order to observe the distribution of out-of-plane spin components, and by subsequent measurements in non-perpendicular geometry for the distribution of the in-plane spin components.

III.1. Exchange bias system: $FeSn_2/Fe$

Maximum information about the spin structure in a bilayer system presenting exchange bias phenomena as obtained by CEMS implies : (i) AF and FM layers containing ^{57}Fe, (ii) epitaxial growth at least of the AF phase, (iii) large magnetic hyperfine splitting in both layers, (iv) high magnetic anisotropy of the AF layer and (v) high T_N . We have found that the $FeSn_2/Fe$ bilayer system fulfils most of the above requirements. The antiferromagnetic $FeSn_2(001)$ phase (D_{4h}, space group I4/mcm, a=0.653 nm and c=0.532 nm) has been epitaxially grown on clean InSb(001) substrates (a=0.647 nm) by MBE (co-evaporation from two sources, 10^{-9} mbar during deposition) [40]. The crystallographic structure and composition were analyzed by RHEED, LEED and AES. Samples with different thicknesses between 15 and 100 nm and with a 30 nm Sn cap layer were obtained for growth temperatures T_s in the range from 150 °C to 300 °C. CEM spectra in perpendicular geometry taken between 80 K and room temperature (RT) on as-grown films revealed T_N values between 200 K and 300 K, depending on the film thickness. For typical thicknesses of 20-30 nm, as usually required in exchange bias systems, T_N approaches 250 K for as-grown samples. By subsequent thermal annealing in UHV T_N increased up to 370 K (Fig. 2). Already after 30 min annealing time a large fraction of the initial paramagnetic phase (cental single line) transforms into a magnetically ordered phase (sextet). X-ray diffraction has shown that this is an optimum annealing time, because for longer annealing the films begin to lose epitaxy. The Mössbauer spectra of the annealed samples show hyperfine fields, B_{hf}, of 10.0(2) T at RT and 15.0(2) T at 80 K. The intensity ratio R_{23} of the magnetic pattern in the room temperature spectra is 4.0(1), in agreement with an in plane alignment of the Fe spins in the AF layer. Bilayer AF/FM systems with ^{57}Fe tracer layers (95% enriched) at the interface were prepared in the sequence:
InSb(001)/$FeSn_2$(20-24 nm)/$^{57}FeSn_2$(4-5 nm)/^{57}Fe(1.2 nm)/Fe(4.8 nm)/Sn(3 nm).

Shifted hysteresis loops were evidenced by SQUID measurements at low temperatures (Fig.3). The exchange bias field B_E, which is about 12 mT (120 Oe) at 5 K, decreases rapidly with temperature and becomes negligible at a much lower temperature

than $T_N = 250$ K, namely around 100 K. Bilayer systems with higher T_N were obtained by appropriate thermal annealing of the AF phase.

Room temperature CEM spectra of an $FeSn_2$/Fe system with $T_N > 400$ K, taken in perpendicular geometry before and after inducing the exchange bias effect, are presented in Fig.4. The exchange bias effect has been induced by cooling the sample in vacuum from 450 K to 320 K (passing through T_N) in the presence of a magnetic field of 1000 Oe applied in the film plane. The Mössbauer spectra were fitted with 3 different sextets. The outer sextets with hyperfine fields of 33.6(3) T and 30.0(3) T are assigned to the Fe atoms in the FM -Fe layer, whereas the inner sextet with a hyperfine field of 10.0(2) T are assigned to Fe atoms in the $FeSn_2$ layer. Since the Mössbauer signal originates only from the tracer layers, it may deduced from the Debye-Waller factor and relative contribution (area) of the considered subspectra that the Mössbauer spectra resolve a first interfacial defected bcc-Fe layer with $B_{hf} = 30.0$ T of only 0.4 nm thickness, a next deeper and less defected 0.8 nm thick bcc-Fe layer ($B_{hf} = 33.6$ T), and the epitaxial 5 nm thick interfacial layer of the AF phase ($B_{hf} = 10.0$ T). Owing to the modest statistics in the CEMS spectra, the spin structure in the first 1.2 nm interfacial -Fe was supposed to be the same. Therefore, the intensity ratios for the two outer sextets were kept the same during the fitting procedure. An intensity ratio R_{23} close to 4 is obtained for these sextets, proving an in-plane spin orientation of the interfacial FM spins both before and after inducing exchange bias. For the interfacial AF spins the R_{23} ratio has decreased from 2.9(1) before field cooling to 2.4(1) after field cooling. Considering the R_{23} value of 4.0(1) for the uncoated AF film, we may conclude that in the AF/FM system the presence of the top FM layer induces an out-of-plane component of the interfacial AF spins, whereas the exchange bias effect enhances this component even more.

Preliminary CEM spectra acquired at room temperature in non-perpendicular geometry (=30°) in a field of 100 mT (above saturation) with the direction of the cooling field along the Oy axis have provided an intensity ratio of $R_{23} = 3.3(1)$ for the interfacial FM iron spins at remanence before inducing the exchange bias (before field cooling) and $R_{23} = 2.7(1)$ after field-cooling the sample through T_N. Within the step-shape angular spin distribution model (homogeneous fan-like spin distribution for the in-plane spin components) [35], the above values show that at remanence and before inducing the exchange bias the FM spins present an angular distribution centered along the saturating field and with a semi-aperture of = 30° After field cooling the angular spin distribution at remanence enlarges substantially towards a semi-aperture of 70°, proving that the in-plane FM spins are preferentially oriented perpendicular to the cooling field, whereby the latter in turn induced the unidirectional anisotropy.

III.2. Exchange spring system: Sm-Co/Fe

The spin configuration in the soft magnetic Fe layer during the magnetic reversal process in the Sm-Co(1100)/Fe bilayer system was investigated by Mössbauer spectroscopy. The bilayers were prepared via dc magnetron sputtering onto a MgO single-crystal with Cr as buffer and cap layer [31] in the sequence MgO(110)/Cr(20 nm)/Sm-Co(10 nm)/^{57}Fe(15 nm)/Cr(5 nm). The epitaxial relationship for Sm-Co(1100) is given by Sm-Co[0001] ||Cr[011] ||Mg[001]. Longitudinal magneto-optic Kerr effect (MOKE) measurements taken with the applied field parallel to the Sm-Co easy axis

(parallel to Mg[001]) yield typical hysteresis loops with exchange fields B_{ex} of 0.15(5) T and switching fields B_{irr} approaching 0.70(5) T [41].

The in-plane spin configuration in the ^{57}Fe layer (95% enriched) was investigated at room temperature by CEMS in applied fields up to 0.9 T. The -radiation was incident under = 20° vs. the sample plane and with the in-plane field orientated along Oy (Fig.1). CEM spectra taken at normal incidence for different applied fields revealed only one magnetic phase assigned to bcc Fe with complete in-plane alignment of the Fe spins (R_{23} 4). Contrary, in non-perpendicular geometry, the Mössbauer spectra exhibit a sensible variation of the intensity ratio vs. the applied magnetic field. Some typical CEM spectra taken in the range of negative fields are shown in Fig.5, whereas the evolution of the intensity ratio R_{23} in Mössbauer spectra vs. the applied field is presented in Fig.6. It may be observed in Fig.6 that the intensity ratio R_{23} decreases from nearly 4 at the highest positive field to a minimum value of 1.5(1) at a critical negative field of B_{cr} = –0.35 T and then increases again at higher negative fields. The results may be interpreted [41] in the frame of the step-shape angular distribution model (fan-like in-plane spin distribution), assuming that the spins in the soft magnetic layer are uniformly distributed inside a field-dependent aperture. This is in agreement with a spiral Fe spin structure, where the rotation angle of the spins in the Fe layer increases with the distance from the hard layer.

In a first approximation we assumed that the first interfacial spins in the soft layer are pinned along their initial Oy direction (along the positive saturation field) up to the critical field B_{cr}. Then, comparison with the theoretical R_{23} ratio demonstrates that the spin distribution aperture starts from 0° at the highest positive field (all the spins aligned along the field direction), and increases to a maximum value of 120° which is reached at the critical field B_{cr}. However, the monotonic steep rise of R_{23} observed between B_{cr} = -0.35 T and B_{ext} = -0.9 T in Fig. 6 cannot be described by a further simple increase of the aperture up to 180° in this model, as a non-monotonic R_{23} behavior is expected for this case [41]. The model should be relaxed in the form of a spiral spin model, where interfacial Fe spins begin to rotate substantially at small negative applied fields down to B_{cr} = -0.35 T, and simultaneously the aperture in the Fe layer increases under the action of the negative field. Then, the sharp rise in R_{23} below B_{cr} = 0.35 T may originate from a decrease of the distribution aperture. Preliminary CEM studies [41] on interfacial ^{57}Fe probe layers in Sm-Co/Fe confirmed the interfacial Fe spin rotation. This means that the spin rotation process for small negative fields extends into the hard magnetic layer, in agreement with recent calculations [31, 34].

IV. Conclusions

After a brief review of exchange bias and exchange spring behavior the potential of the ^{57}Fe probe layer technique in Mössbauer spectroscopy (CEMS) for the spin structure determination in these layered systems is described. If the incident -radiation is perpendicular to the film plane (perpendicular geometry) spin components perpendicular to the plane may be obtained from the line intensity ratio whereas the spectra are insensitive to the in-plane spin configuration. As an example, epitaxially grown antiferromagnatic (AF) $FeSn_2$ (001) films are shown to have an in-plane spin structure. However, coating with a layer of FM polycrystalline bcc Fe in its remanent state induces

an out-of-plane component of the interfacial AF spins. Evidence is provided for an enhancement of this effect when exchange bias is induced by field cooling, although the interfacial FM spins remain oriented in the film plane.

The spin configuration with predominantly in-plane Fe spins may be analyzed in non-perpendicular geometry with the -radiation incident at an angle 90° relative to the film plane. This is demonstrated for the Sm-Co/Fe spring magnet. CEM spectra taken in an external field show a remarkable change in the line intensity ratio arising from the in-plane spiral Fe spin structure within the magnetically soft Fe film during the magnetic reversal process. Our data provide evidence for a spin rotational process extending into the hard magnetic layer.

[*] Permanent address: National Institute for Physics of Materials, P. O. Box MG7, RO-76900 Bucharest – Magurele, Romania

[**] Permanent address: Department of Materials Science and Engineering, Nagoya University, Nagoya, Japan

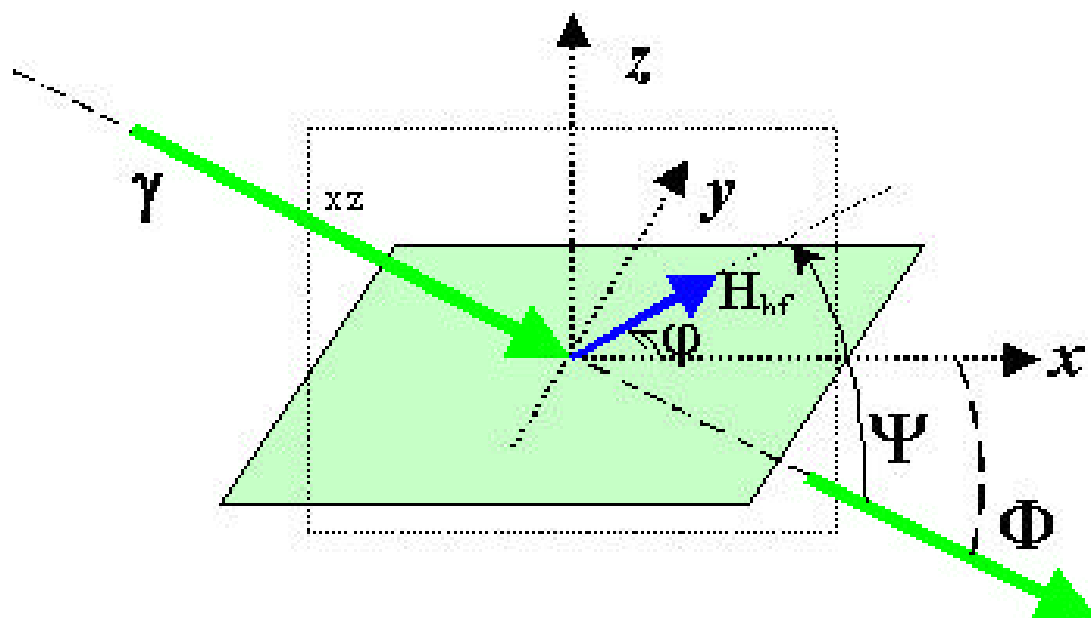Permanent address: Faculty of Physics, Dicle University, Diyarbakir, Turkey

References

1. W.H. Meiklejohn and C.P. Bean, Phys. Rev. 102 (1956) 1413
2. S. Gangopadhyay, G.C. Hadjipanayis, C.M. Sorensen and K.J. Klabunde, IEEE Trans. Magn. 28 (1992) 3174
3. V. Papaefthymiou, A. Kostikas, A. Simopulos, D. Niarchos, S. Gangopadhyay, G.C. Hadjipanayis, C.M. Sorensen and K.J. Klabunde, J. Appl. Phys. 67 (1990) 4487
4. A.A. Glazer, A.P. Potapov and R.I. Tagirov, Sov. Phys. JETP. Lett. 15 (1972) 259
5. R.D. Hempstead, S. Krongelb and D.A. Thompson, IEEE Trans. Magn. 14 (1978) 521
6. A.J. Devasahayam, K.R. Mountfield and M.H. Kryder, IEEE Trans. Magn. 33 (1997) 2881
7. T. Lin, G.L. Gorman and C. Tsang, IEEE Trans.Magn. 32 (1996) 3443
8. J. Fujikata, K. Hayashi, H. Yamamoto and K. Yamada, J.Magn.Soc.Japan 19 (1995) 365
9. J.C.S. Kools, IEEE Trans.Magn. 32 (1996) 3165
10. B. Dieny, V.S. Speriosu, S.S.P. Parkin, B.A. Gurney, D.R. Wilhoit and D. Mauri, Phys.Rev. B 43 (1991) 1297
11. B. Dieny, J. Magn. Magn. Mater. 136 (1994) 335
12. J. Nogues and I.K. Schuller, J. Magn. Magn. Mater. 192 (1999) 203
13. R. Coehoorn, D.B. de Mooji, J.P.W.B. Duchateau and K.H.J. Buschow, J. Phys. 49 (1988) C8-669
14. E.F. Kneller and R. Hawig, IEEE Trans. Magn. 27 (1991) 3588
15. R. Skomski and J.M.D. Coey, Phys. Rev. B48 (1993) 15812
16. R. Fischer, T. Leineweber and H. Kronmüller, Phys. Rev. B57 (1998) 10723
17. T. Schrefl and J. Fidler, IEEE Trans. Magn. 35 (1999) 3223
18. W.H. Meiklejohn and C.P. Bean, Phys. Rev. 105 (1957) 904
19. W.H. Meiklejohn, J. Appl. Phys. 33 (1962) 1328
20. L. Neel, Ann. Phys.(Paris) 2 (1967) 61
21. D. Mauri, H.C. Siegmann, P.S. Bagus and E. Kay, J. Appl. Phys. 62 (1987) 3047
22. A.P. Malozemoff, J. Appl. Phys. 63 (1988) 3874
23. T.J. Moran and I.K. Schuller, J. Appl. Phys. 79 (1996) 5109
24. Y. Ijiri, J.A. Borchers, R.W. Erwin, S.H. Lee, P.J van der Zaag and R.M. Wolf, Phys. Rev. Lett. 80 (1998) 608
25. N.C. Koon, Phys. Rev. Lett. 78 (1997) 4865
26. T.C. Schulthess and W.H. Butler, Phys. Rev. Lett. 81 (1998) 4516; T.C. Schulthess and W.H. Butler, J. Appl. Phys. 85 (1999) 5510
27. U. Nowak, A. Misra, and K.D. Usadel, J. Appl. Phys. 89 (2001) 7269
28. Y. Ijiri, J.A. Borchers, R.W. Erwin, S.H. Lee, P.J. van der Zaag and R.M. Wolf, Phys. Rev. Lett. 80 (1998) 608
29. H. Ohldag, A. Scholl, F. Nolting, S. Anders, F.U. Hillebrecht and J. Stohr, Phys. Rev. Lett. 86 (2001) 2878
30. E. Goto, N. Hayashi, T. Miyashita and K. Nakagawa, J. Appl. Phys. 36 (1965) 2951
31. E.E. Fullerton, J.S. Jiang, M. Grimsditch, C.H. Sowers and S.D. Bader, Phys. Rev. B 58 (1998) 12193
32. K. Mibu, T. Nagahama and T. Shinjo, J. Magn. Magn. Mater. 163 (1996) 75
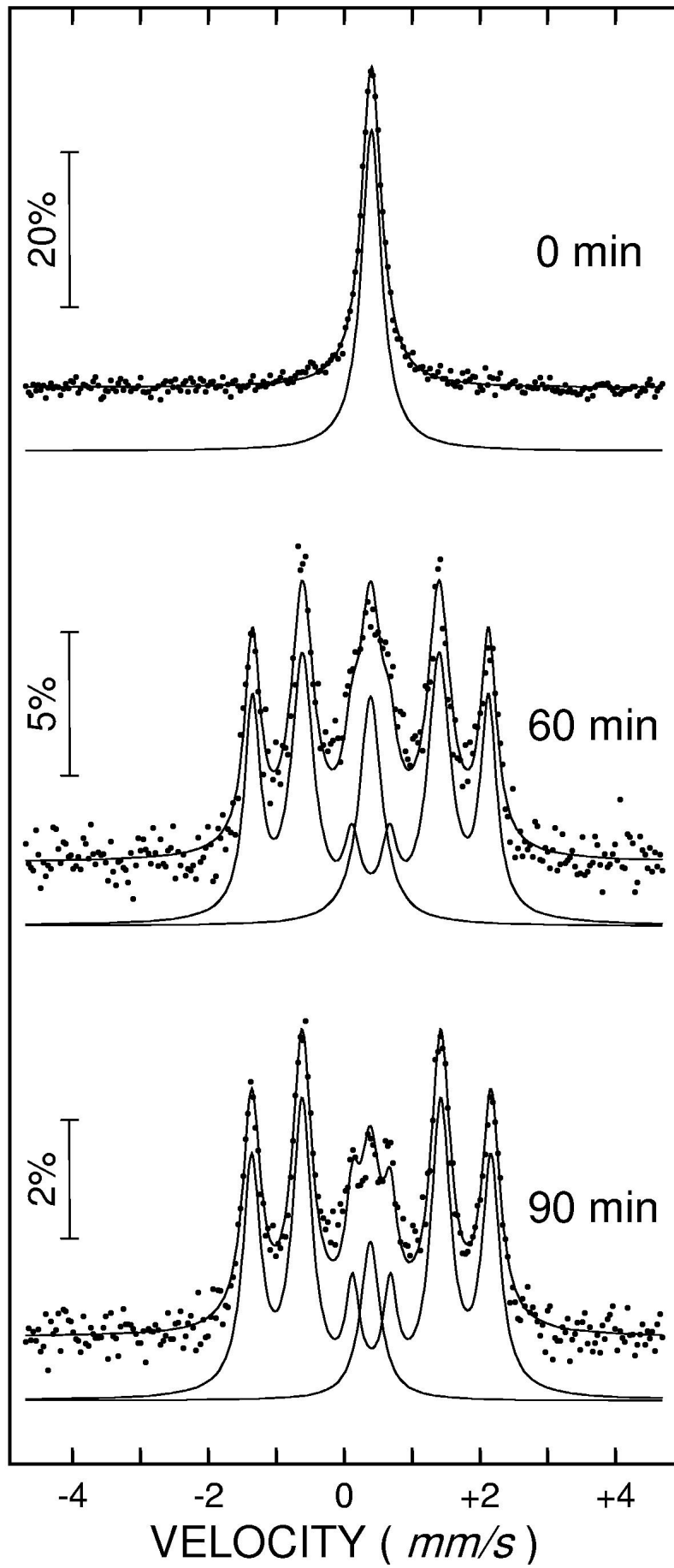
33. T. Nagahama, K. Mibu and T. Shinjo, J. Phys. D 31 (1998) 43
34. K. Mibu, T. Nagahama, T. Shinjo and T. Ono, Phys. Rev. B 58 (1998) 6442
35. Ch. Sauer and W. Zinn, in: L.H. Bennett and R.E. Watson (eds.), Magnetic Multilayers, World Scientific, Singapore, 1993
36. M. Przybylski, Hyperfine Int. 113(1998)135
37. T. Shinjo and W. Keune, J. Magn. Magn. Mater. 200(1999)598
38. G.K. Wertheim, Mössbauer Effect: Principles and Applications, Academic Press, New York, 1964
39. V. Kuncser, W. Keune, M. Vopsaroiu and P.R. Bissell, submitted to Nucl. Instr. and Meth. in Phys. Res. B
40. V. Kuncser, M. Doi and W. Keune (unpublished)
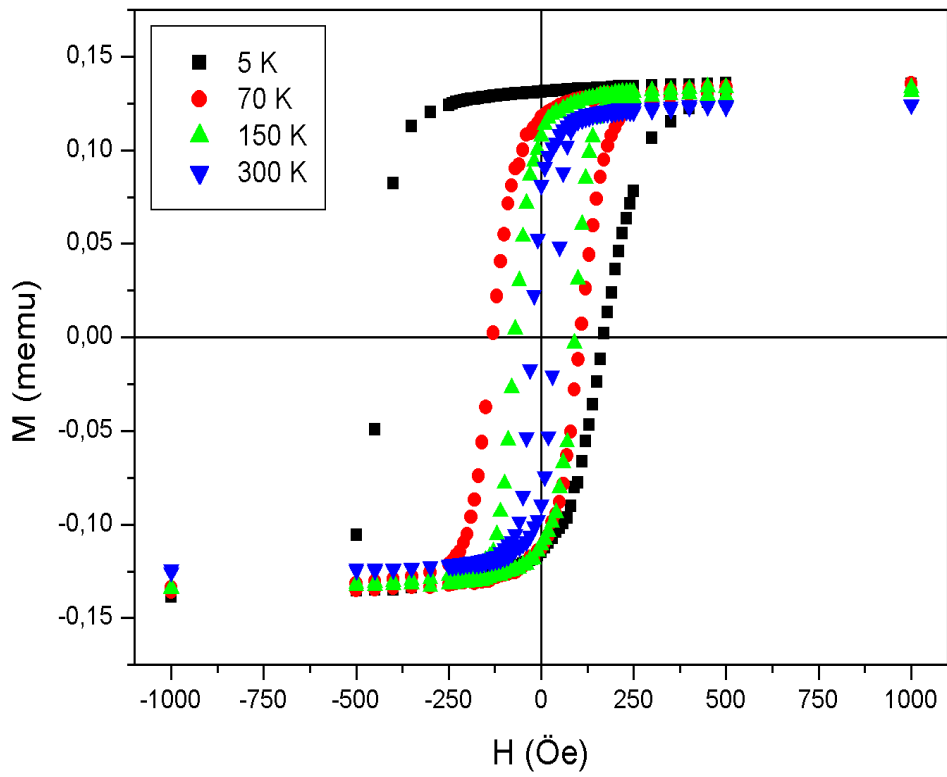41. V. Kuncser, M. Doi, M. Askin, H. Spies, B. Sahoo, W. Keune, J.S. Jiang and S.D. Bader (unpublished)

Figure captions

Figure 1:   Geometrical arrangement of a CEMS experiment in non-perpendicular geometry.

Figure 2:   Room-temperature CEM spectra (taken in perpendicular geometry, = 0°) of 300 nm thick $^{57}FeSn_2(001)$ film grown at T_s = 200 °C (top, as grown) and after annealing at 350 °C for 60 min and 90 min, respectively. (sample # af2).

Figure 3:   SQUID magnetization loops of exchange-biased $FeSn_2$(28 nm)/(Fe(6.2 nm) bilayer (as grown, T_S = 200 °C, T_N 250 K), taken at different temperatures. (sample # eb1).

Figure 4:   CEM spectra of [$FeSn_2$(20 nm)/$^{57}FeSn_2$(5 nm)/^{57}Fe(1.2 nm)/Fe(4.8 nm)] bilayer with T_N > 400 K). The spectra were taken at RT in perpendicular geometry (= 0°) before (initial) and after (final) field cooling through T_N. (sample # eb3).

Figure 5:   Room-temperature CEM spectra of Sm-Co(10 nm)/^{57}Fe(15 nm) spring magnet, taken at different values of the (negative) in-plane applied field. Right-hand side: extracted hyperfine-field distributions, $P(B_{hf})$.

Figure 6:   Mössbauer line intensity ratio R_{23} as a function of decreasing (in-plane) external field. The measurement started at B_{ex} = +0.9 T and finished at B_{ext} = -0.9 T.

initial

final

0.5%

2%

RELATIVE EMISSION

VELOCITY (*mm/s*)

-8   -4   0   +4   +8